



Journal Name

COMMUNICATION

Demonstration of an Azobenzene Derivative based Solar Thermal Energy Storage System

Zhihang Wang,^a Raul Losantos,^b Diego Sampedro,^{*b} Masa-aki Morikawa,^{cd} Karl Börjesson,^e Nobuo Kimizuka^{*cd} and Kasper Moth-Poulsen^{*a}

Received 00th January 20xx,
Accepted 00th January 20xx

DOI: 10.1039/x0xx00000x

www.rsc.org/

Molecules capable of reversible storage of solar energy have recently attracted increasing interest, and are often referred to as molecular solar thermal energy storage (MOST) systems. Azobenzene derivatives have great potential as an active MOST candidate. However, an operating lab scale experiment including solar energy capture/storage and release has still not been demonstrated. In the present work, a liquid azobenzene derivative is tested comprehensively for this purpose. The system features several attractive properties, such as a long energy storage half-life (40 h) at room temperature, as well as an excellent robustness demonstrated by optically charging and discharging the molecule over 203 cycles without any sign of degradation (total operation time 23 h). Successful measurements of solar energy storage under solar simulated sunlight in a microfluidic chip device have been archived. The identification at testing of two heterogenous catalyst system enabled the construction of a fixed bed flow reactor demonstrating catalyzed back conversion from *cis* to *trans* azobenzene at room temperature under flow conditions. The working mechanism of the more suitable catalytic candidate was rationalized by detailed density functional theory (DFT) calculations. Thus, this work provides detailed insights into the azobenzene based MOST candidate and identifies where the

system has to be improved for future solar energy storage applications.

Introduction

The development of sustainable energy attracts increasing attention, due to the pressing environmental and societal challenges linked to high dependency of fossil fuels in our modern society.¹ As the most abundant energy source for Earth, the sun can provide the energy needed by humankind for an entire year in only six hours.² Various ways to take advantage of solar energy have been studied and developed over last decades, including photovoltaics,³ artificial photosynthesis,⁴ as well as solar thermal heating.⁵ In order to store sun light for future use, molecular solar thermal storage techniques (MOST^{6,7} also known as solar thermal fuels, STF⁸) focus on harvesting solar energy and storing it in photoswitchable materials. A parent molecule can be isomerized by solar irradiation to a metastable high energy photoisomer for a long storage period. When the energy is required, it can be thermally or catalytically back converted to the parent state. Ideally, the stored energy should be released on-demand as heat, thus operating as a closed-cycle system.

In order to realize the MOST concept, several features concerning the charge and discharge process need to be considered.^{7,9,10} 1) Since more than 50% of the sun light is distributed from 300 nm to 800 nm, the parent molecules should be able to absorb broadly in this spectral region. 2) The quantum yield of the photoisomerisation reaction should be as close to unity as possible. 3) The storage half-life at room temperature should be long enough to fulfill application relevant storage times, such as daily, monthly, yearly or even longer storage requirements. 4) The energy of the metastable photoisomer should be significantly higher than the ground state of the parent isomer. 5) The system should ideally be able to operate over an infinite number of charging and heat releasing cycles. 6) Using a heterogeneous catalyst, the

^a Department of Chemistry and Chemical Engineering, Chalmers University of Technology, 41296 Gothenburg, Sweden.
E-mail: kasper.moth-poulsen@chalmers.se

^b Department of Chemistry, Centro de Investigación en Síntesis Química (CISQ), Universidad de La Rioja, Madre de Dios 53, E-26006 Logroño, La Rioja, Spain.
E-mail: diego.sampedro@unirioja.es

^c Department of Chemistry and Biochemistry, Graduate School of Engineering, Kyushu University, 744 Moto-oka, Nishi-ku, Fukuoka 819-0395, Japan.

^d Center for Molecular Systems (CMS), Kyushu University, 744 Moto-oka, Nishi-ku, Fukuoka 819-0395, Japan.

^e Department of Chemistry and Molecular Biology, University of Gothenburg, Kemigården 4, 41296 Gothenburg, Sweden
E-mail: kimizuka.nobuo.763@m.kyushu-u.ac.jp

† Electronic Supplementary Information (ESI) available: [details of any supplementary information available should be included here]. See DOI: 10.1039/x0xx00000x

photoisomer should easily release the stored energy as heat. 7) For energy collection, storage, as well as bulk heating applications, MOST materials need to be pumped between solar collector, storage reservoir and heat extraction devices. As a consequence, the MOST system should be a liquid or highly soluble solid.

The MOST concept has been represented by many potential candidates, including norbornadiene/quadracyclane derivatives,^{7,9-14} the dihydroazulene/vinylheptafulvene couple,¹⁵⁻²¹ difulvalenediruthenium complexes,⁶ anthracene dimerization,²² Dewar isomer²³ as well as azobenzene derivatives.^{8,24-43} The latter systems have been in the spotlight recently due to the broad absorption spectrum, high robustness, daily storage half-life, tunable energy density (J mol⁻¹) of the photoswitches, as well as the low synthetic cost.⁴⁰⁻⁴² **AZO1**, (see Figure 1. a) possesses many of the needed features as described above, however it has not been tested in a full MOST operating cycle including energy capture, storage and release. Here, for the first time, we investigate the performance of **AZO1** by studying its function through multiple energy storage and release cycles. In order to do so, we have identified and tested a heterogeneous catalyst system for the energy release step and constructed a flow system consisting of a solar collector and a fixed-bed catalytic converter. Further, the functioning mechanism of the catalytic conversion is further proposed and rationalized using PCM-B3LYP-D3BJ/6-31G(d)+SDD(Cu) calculations.

Results and discussion

To characterize the physical properties of **AZO1**, it was firstly studied in toluene in terms of its absorptivity, half-life of energy storage and quantum yields of photoisomerization reaction. Comparing these results with available data of **AZO1** in methanol,⁴³ the maximum in the absorption spectrum was observed to be slightly red shifted, indicating a low solvent polarity effect compared to, for instance, the DHA-MOST system¹⁸ (ca. 5 nm, $\epsilon_{\text{Max}@350\text{nm}} = 2.6 \times 10^4 \text{ M}^{-1} \text{ cm}^{-1}$, see Figure 1. b). Concerning the storage lifetime, a half-life from *cis* to *trans* state of 36.3 h in toluene can be extracted from the Eyring plot. The activation enthalpy was calculated as $\Delta H^\ddagger_{\text{therm}} = 93.7 \text{ kJ mol}^{-1}$, together with an activation entropy $\Delta S^\ddagger_{\text{therm}} = -31.7 \text{ J mol}^{-1} \text{ K}^{-1}$. (Supplementary S2, ESI[†]). The quantum yield of the *trans* to *cis* photoisomerisation reaction was determined to be 21% at 340 nm, using a literature procedure⁴⁴ (Supplementary S3, ESI[†]). In addition, it was observed that the **AZO1-cis** state can photoisomerise back to the *trans* form. The corresponding quantum yield of the *cis* to *trans* photoisomerisation was determined to be 23% at 455 nm, slightly higher than the reverse process. Due to this photo-induced double switch effect for **AZO1**, full conversion via full spectrum solar light can likely not be achieved and a band pass filter was used in the device conversion experiments.

Good cyclability is one of the most important criteria of MOST systems. To investigate the robustness of **AZO1**, a solution of ca. 10⁻⁵ M in toluene was prepared without degassing. Two controllable LED light sources were turned on and off

alternatingly (340 nm with 100 s irradiation time, 455 nm with 300 s irradiation time) to charge and discharge the molecules back and forth. After 203 complete cycles (with a total operation time of 22.6 h), no significant signs of degradation were observed, thus demonstrating a high robustness of **AZO1**, even in the presence of oxygen (see Figure 1. c).

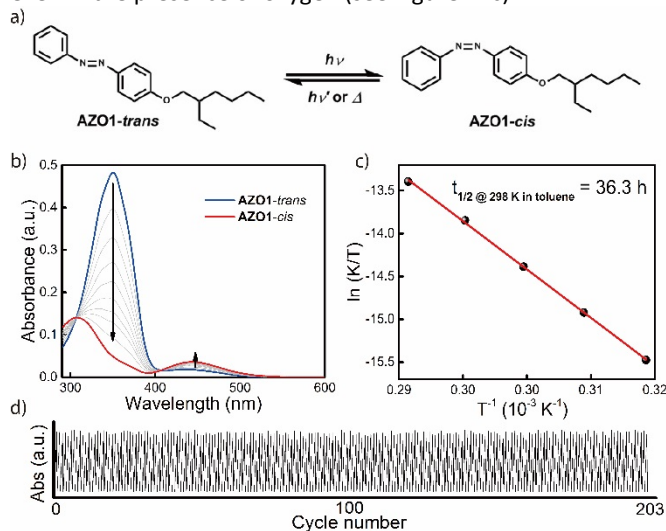


Fig 1. a) Structure of **AZO1** in *trans* and *cis* state. b) Absorption spectra of **AZO1-trans** (in blue) and its corresponding photoisomer **AZO1-cis** (in red). The sample (ca. 2 mg into 100 mL toluene) was converted with a 340 nm LED lamp. c) Eyring plot of **AZO1-cis**. The half-life at 25 °C was determined as 36.3 h in toluene solution. d) Optical cycling test of **AZO1** in toluene. The figure shows 203 cycles in total. The absorbance was recorded at 350 nm. The charge and discharge processes were archived with a 340 nm LED (~60 mW) over 100 s and a 455 nm LED (~1020 mW) over 300 s, alternatively.

To further demonstrate the functionality of the **AZO1** system in a real device, a continuous flow system was built. For this lab-scale conversion test under an AM1.5 solar simulator, diluted solutions of **AZO1** were used to allow data collection by UV-Vis spectroscopy. Two concentrations of **AZO1** solutions were pumped individually through a microfluidic chip,^{20,21} with varying residence time (33.9 mm³ inner volume with a channel depth of 100 μm , see Figure 2. a). Since **AZO1-cis** can be back-converted by visible light, an optical UV transmitting band pass filter (<400nm) was inserted in between the solar simulator and the microfluidic chip. The UV-Vis spectra of the **AZO1** solution before and after the microfluidic chip were measured. Equation 1 was used to calculate the *cis*-to-*trans* conversion percentage (Supplementary S4, ESI[†]):

$$\text{Conversion \%} = \frac{A_{@350 \text{ nm}}}{A_{\text{iso}@306 \text{ nm}}} \cdot \frac{\epsilon_{\text{iso}@306 \text{ nm}} - \epsilon_{\text{isomer}@350 \text{ nm}}}{\epsilon_{\text{parent}@350 \text{ nm}} - \epsilon_{\text{isomer}@350 \text{ nm}}} \quad (1)$$

Where $A_{@350 \text{ nm}}$ is the actual absorbance at 350 nm; $A_{\text{iso}@306 \text{ nm}}$ and $\epsilon_{\text{iso}@306 \text{ nm}}$ correspond to the absorbance and absorptivity of the solution at its isosbestic point at 306 nm, respectively; and $\epsilon_{\text{parent}@350 \text{ nm}}$ and $\epsilon_{\text{isomer}@350 \text{ nm}}$ are the absorptivity of the **AZO1-trans** and **AZO1-cis** isomers at 350 nm, respectively. A maximum conversion of around 80% from **AZO1-trans** to *cis* state was obtained from a solution of $2 \times 10^{-4} \text{ M}$. This is likely due to the photo-stationary state

of azobenzene *trans*-to-*cis* photoisomerization (see Figure 2. b). Concerning the energy storage efficiency, 0.88% of the solar energy could theoretically be stored in a neat sample (Supplementary S5, ESI†). The highest efficiency that can be researched for 5×10^{-4} M solution is 0.02%, and for 2×10^{-4} M solution is 0.01%. With a band pass filter (SCHOTT, UG11) and a solar simulator, the actual measurements showed that the maximum energy storage efficiency was determined as *ca.* 0.009% for the 5×10^{-4} M solution, and 0.005% for the 2×10^{-4} M solution (see Figure 2. c, Supplementary S6, ESI†). Those experimental results were promising to reach the theoretical predictions, but are still overall limited by concentrations and photo-stationary state between the two species.

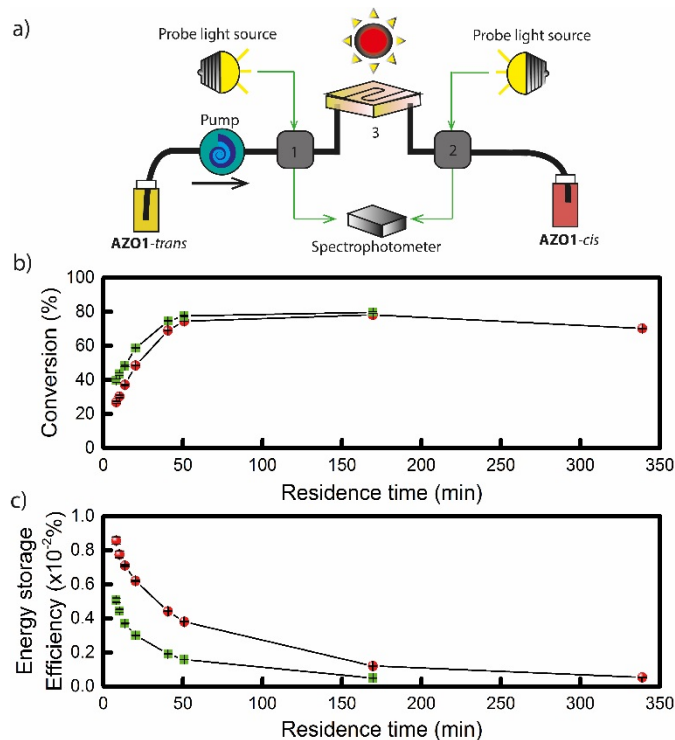


Fig 2. a) Experimental setup of **AZO1** in a fluidic chip device. Gray boxes 1 and 2 contain a flow UV-Vis detection device connected to a portable spectrophotometer, 3, corresponding to a total volume of 33.9 mm³ quartz chip, with a 100- μ m optical path length. **b)** Experimental data of two concentrations used: 2×10^{-4} M in green, and 5×10^{-4} M in red. Conversion percentage of **AZO1-trans** with different residence times in the microfluidic chip. **c)** Measured energy storage efficiency of the **AZO1** compound in toluene.

After solar capture/storage, energy release is the second fundamental process for MOST concept. To estimate the adiabatic heat release as a function of concentration, a modified equation from previous work¹¹ has been used (equation 2):

$$\Delta T = \frac{c \cdot M_w \cdot \Delta H_{storage}}{\frac{c^2 \cdot M_w^2}{\rho_{AZO1}} \cdot C_{p,AZO1} + \left(1 - \frac{c \cdot M_w}{\rho_{AZO1}}\right) \rho_{solvent} \cdot C_{p,solvent}} \quad (2)$$

where c is the concentration of **AZO1**, M_w represents its molecular weight; $\Delta H_{storage}$ corresponds to the DSC measured energy storage capacity of **AZO1-cis** which equals to 167.5 J g⁻¹; $C_{p,AZO1}$ is the specific

heat capacity of **AZO1** in J g⁻¹ K⁻¹, assuming similar as unsubstituted azobenzene⁴⁵; and $\rho_{solvent}$ and $C_{p,solvent}$ address the volumetric mass density in g L⁻¹ and the specific heat capacity in J g⁻¹ K⁻¹ of the solvent, respectively (which are equal to 867 g L⁻¹ and 1.7 J g⁻¹ K⁻¹). In this approach, the volume load factor of the solvent and photoisomer were considered, i.e. when the concentration approaches neat conditions, the $\left(1 - \frac{c \cdot M_w}{\rho_{AZO1}}\right) \rho_{solvent} \cdot C_{p,solvent}$ approaches to zero. This correction is reasonable for all MOST heat release estimations with close to neat conditions. In the case of **AZO1**, the theoretical maximum temperature difference was calculated as *ca.* 226 °C for a fully charged neat sample (see Supplementary S7, ESI†).

Concerning related catalysts, several candidates, including mineral acids like perchloric acid, Cu(II) salts (CuCl₂, Cu(OAc)₂), gold nanoparticles which involve a redox mechanism, as well as electrocatalytic method have been reported to induce the back conversion of azobenzene derivatives.⁴⁶⁻⁴⁸ However, for a closed cycle system which can be operated in devices, a heterogeneous catalyst that can be fixed in a reaction centre is required. Based on this fact, a heterogeneous catalyst or an insoluble homogeneous catalyst needs to be developed. For **AZO1**, two potential catalysts, cobalt(II) phthalocyanine physisorbed on the surface of activated carbon (CoPc@C) and [Cu(CH₃CN)₄]PF₆ fulfill the described physical properties and thus, they were tested individually. Both showed a positive effect on reducing the back conversion half-life at room temperature. [Cu(CH₃CN)₄]PF₆ has a very low solubility in toluene, being active for various MOST systems, including norbornadiene/quadracyclane derivatives¹¹ as well as the dihydroazulene/vinylheptafulvene couple.^{20,49} For **AZO1-cis** compound, it was calculated as up to 30 s⁻¹ back conversion reaction rate at room temperature of 25 °C. (up to 6×10^6 time higher compared to a reaction rate of 5×10^{-6} s⁻¹ without catalyst at 25 °C, see Figure 3. a, Supplementary S7, ESI†). CoPc@C was produced following the reported procedure, however risk to leach from its solid support.¹¹ Therefore, the [Cu(CH₃CN)₄]PF₆ salt was chosen to be incorporated in the catalytic device for further testing. With this result in mind, a small-sized reaction centre was built. 5 mg of the Cu(I) salt was inserted into a Teflon tube which has a 1 mm inner diameter (see Figure 3. b). 5×10^{-4} M of 79% **AZO1-cis** solution from microfluidic chip experiments was then flowed through the catalytic bed with a speed of 1 mL h⁻¹. As result, 48% of the **AZO1-cis** was successfully back converted to the corresponding *trans* state. Thus, the described continuous fluidic chip experiments can achieve the requirements for a complete application of the MOST concept including photon capture/storage and energy release process.

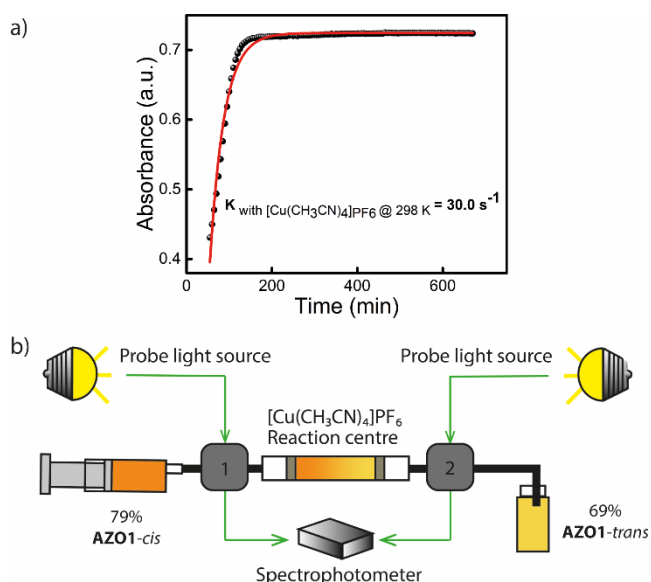


Fig 3. a) Kinetics study of **AZO1-cis** in presence of $[\text{Cu}(\text{CH}_3\text{CN})_4]\text{PF}_6$ in toluene at $25\text{ }^\circ\text{C}$. Black dots represent the experimental data, red curve corresponds to the exponential fitting. The reaction constant was calculated as 30.0 s^{-1} **b)** Conceptual device demonstration of catalytic back conversion of **AZO1-cis**. Around 5 mg of Cu(I) salt were loaded in to the reaction centre. A $5 \times 10^{-4}\text{ M}$ 79% **AZO1-cis** solution was flown through the Cu(I) reactor with a speed of 1 mL h^{-1} . 69% of the **AZO1-trans** was obtained after the reaction centre, i.e. 48% of the **AZO1-cis** can be successfully back converted to **AZO1-trans** state.

To further understand the mechanism of back-conversion with $[\text{Cu}(\text{CH}_3\text{CN})_4]\text{PF}_6$, a detailed study within the framework of the density-functional theory (DFT) was performed. A simplified **AZO1** system was used replacing the ethylhexyl moiety with a methyl group at the PCM-B3LYP-D3BJ/6-31G(d)+SDD(Cu) level of theory (Supplementary S8, ESI[†]). Among the different coordination options, the CH_3CN ligands could be displaced by the new ligand (the *cis* isomer of the azobenzene moiety, in this case). Four different coordination possibilities were considered to ensure a good modelling of the experimental conditions. In all cases, the formation of the new complex is slightly endergonic ($1\text{--}5\text{ kcal mol}^{-1}$). As the azobenzene derivative is not symmetric, two sets of coordination alternatives arise. Coordination through the nitrogen atom directly linked to the unsubstituted phenyl ring (path b, Supplementary S8, ESI[†] and Figure 4. a) is favored (by *ca.* 2.3 kcal mol^{-1}) as compared to the methoxyphenyl linked nitrogen atom (path a). Isomerization of azobenzenes is very dependent on substitution and reaction conditions.⁵⁰ In this case, different pathways were considered and rotation and inversion mechanisms of the isomerization were explicitly evaluated. As in the not catalyzed thermal reaction,⁴⁷ the inversion transition states (**TS1a-TS1b**) were found to be preferred.

A relaxed scan along the rotation coordinate (CNNC dihedral) (see Figure 4. b) reveals a possible $\text{S}_0\text{-T}_1\text{-S}_0$ mechanism accessible by coordination of the nitrogen atom of **AZO1-cis** to copper, which reveals a MLCT (metal-to-ligand charge transfer). In turn, this implies the participation of a π^* orbital of the azobenzene allowing rotation along the $\text{N}=\text{N}$ with participation of the T_1 state. At relative high torsion angles, the triplet state becomes less energetic and this path

yields a barrier of around 20 kcal mol^{-1} . This alternative mechanism allows for the bypassing of the more energetic inversion TS in the ground state (30 kcal mol^{-1}) and it should be available at room temperature.

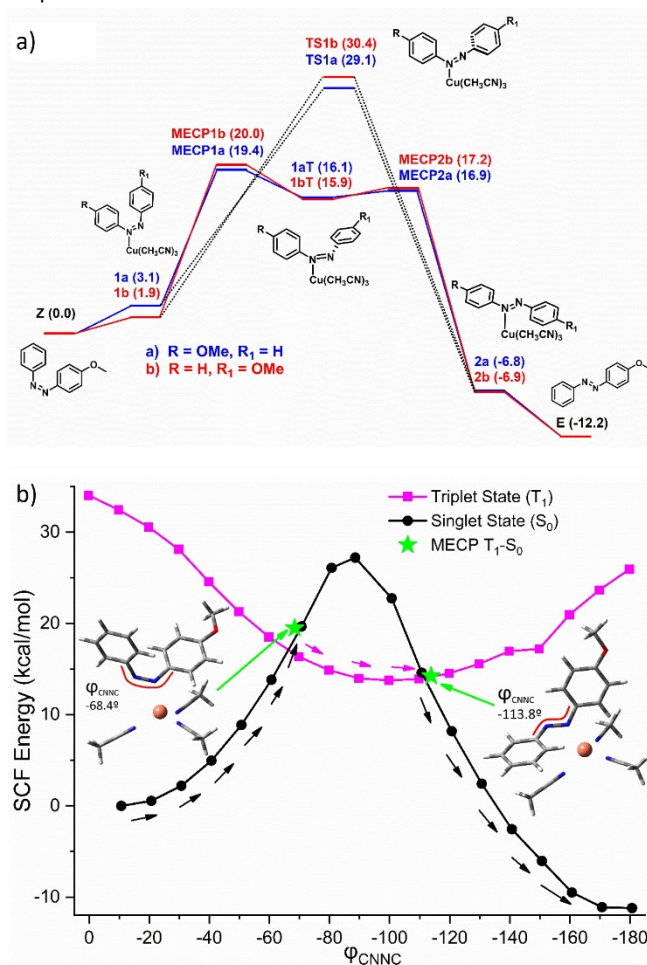


Figure 4. a) Reaction paths for *cis-trans* isomerization. Coordination through the nitrogen atom directly linked to the phenyl ring (path b, in red) and to the methoxyphenyl nitrogen atom (path a, in blue). Solid lines are the $\text{S}_0\text{-T}_1\text{-S}_0$ pathway (MECP1(a,b)-1(a,b)T-MECP2(a,b)). Dotted black lines are the singlet reaction path (TS1a-TS1b). Free energies referred to *cis*-AZO+Cu(CH₃CN)₄⁺. **b)** Relaxed scan along CNNC rotation and MECPS.

Thus, copper coordination yields a decrease in the isomerization barrier of *ca.* 6 kcal mol^{-1} (computed barrier decreases from $25.4\text{ kcal mol}^{-1}$ for free azobenzene to $19.4\text{ kcal mol}^{-1}$). This relatively small decrease in the energy barrier is enough to allow the isomerization process to occur in few minutes instead of some days, thus accelerating the isomerization by 4 orders of magnitude, allowing a good agreement with experiments (energy difference of 8 kcal mol^{-1} , from $23.5\text{ kcal mol}^{-1}$ for the free **AZO1** to $15.6\text{ kcal mol}^{-1}$ for the copper activated reaction). Overall, while $[\text{Cu}(\text{CH}_3\text{CN})_4]\text{PF}_6$ is useful to increase notably the reaction rate, there is still great potential for improvement in the design of the energy release step. This could be done, for instance, favoring the MLCT or stabilizing the MECP between singlet and triplet states to increase the efficiency of the crossing. In both cases, this could lead to a decrease in the energy barrier and a subsequent acceleration of the back-conversion.

Conclusions

An **AZO1**-MOST charging/discharging cycle has been successfully demonstrated, including the study of the photophysical properties and the back-conversion of the photoisomer. The **AZO1** system features a strong absorption ($\epsilon_{\text{Max@350nm}} = 2.6 \times 10^4 \text{ M}^{-1} \text{ cm}^{-1}$) and high thermal half-life (36.3h). The optical cyclability test for a diluted solution shows no significant degradation in the presence of oxygen, allowing the use of **AZO1** in toluene in application. For MOST application purposes, the conversion quantum yield at 340 nm was determined to be 21% which is similar to the quantum yield of back conversion of 23% at 455 nm. This implies that even diluted samples cannot be fully converted under sun light. The estimated maximum energy storage efficiency for **AZO1** in neat state was calculated to be 0.88%. To experimentally demonstrate the functionality of this liquid azobenzene for MOST applications, different concentrations of **AZO1** conversion experiments were performed in a continuous microfluidic chip system. The measured maximum energy storage efficiency for a solution of $5 \times 10^{-4} \text{ M}$ can reach close to 0.009%, promising to reach the theoretical prediction of 0.02% at such concentration. This, unfortunately, showed a strong photo-stationary effect between **AZO-cis** and **AZO-trans**. This highlights the need to work with altering the optical properties of the azobenzene system.^{51–53} Further improvement to increase quantum yields and to diminish the absorption of photoisomer, as well as differentiate the spectra difference between *cis* and *trans* states would be certainly required. To estimate the theoretical heat release temperature difference, a corrected formula was introduced to account for the change from diluted solution to neat sample. **A maximum temperature increase of 226 °C can be theoretically achieved by using equation (2) with correction term for a neat MOST sample.** Furthermore, two new catalysts have been identified to allow the back conversion of **AZO1-cis** and a reaction centre based on a Cu(I) salt has been prepared as a proof of concept for the energy release process. With a concentration of $5 \times 10^{-4} \text{ M}$ and a flow speed of 1 mL h^{-1} , 69% of the *cis* state isomer was successfully converted back to *trans* state. However, the reaction rate was still too low to be used for macroscopic heat release purposes. Finally, a detailed theoretical study of the mechanism has been proposed to further understand the discharge process using a Cu(I) salt. This could help in the future design of new azobenzene derivatives and the corresponding catalysts. In addition, results shown here could be extended to the control of azobenzene derivatives in different applications.

Conflicts of interest

There are no conflicts to declare.

Acknowledgements

This work was supported by the K. & A. Wallenberg foundation and the Swedish Foundation for Strategic Research. D. S. and R. L. thank the Spanish Ministerio de Economía y Competitividad (MINECO)/Fondos Europeos para el Desarrollo Regional (FEDER) (CTQ2017-87372-P). R. L. thanks the Universidad de La Rioja for his fellowship. This work used the Beronia cluster (Universidad de La Rioja), which is supported by FEDER-MINECO grant number UNLR-094E-2C-225. Thanks a lot to Xin Wen and Sarah Lerch for all the fruitful discussions.

Notes and references

- 1 IPCC, *Climate Change Synthesis Report Summary for Policymakers*, 2014.
- 2 R. Perez and M. Perez., *The International Energy Agency SHCP Solar Update*, 2009, **50**, 2–3.
- 3 K. Mertens, *Photovoltaics: Fundamentals, Technology and Practice*, Wiley, 2014.
- 4 F. Collings and C. Critchley, *Artificial Photosynthesis: From Basic Biology and Industrial Application*, Wiley, 2005.
- 5 S.M. Hasnain., *Energy Convers. Manag.*, 1998, **39**, 1127–1138.
- 6 K. Moth-Poulsen, D. Čoso, K. Börjesson, N. Vinokurov, S. K. Meier, A. Majumdar, K. P. C. Vollhardt and R. A. Segalman, *Energy Environ. Sci.*, 2012, **5**, 8534–8537
- 7 Yoshida, Z.-i. *Journal of photochemistry*, 1985, **29**, 27–40.
- 8 L. Dong, Y. Feng, L. Wang and W. Feng, *Chem. Soc. Rev.*, 2018, **47**, 7339–7368
- 9 V. A. Bren', A. D. Dubonosov, V. I. Minkin, V. A. Chernoiyanov, *Russ. Chem. Rev.*, 1991, **60**, 913–948.
- 10 K. Börjesson, A. Lennartson, and K. Moth-Poulsen, *ACS Sustain. Chem. Eng.*, 2013, **1**, 585–590.
- 11 Z. Wang, A. Roffey, R. Losantos, A. Lennartson, M. Jevric, A. U. Petersen, M. Quant, A. Dreos, X. Wen, D. Sampedro, K. Börjesson and K. Moth-Poulsen., *Energy Environ. Sci.*, 2019, **12**, 187–193.
- 12 A. Dreos, Z. Wang, J. Udmark, A. Ström, P. Erhart, K. Börjesson, M. B. Nielsen and Kasper Moth-Poulsen, *Adv. Energy Mater.*, 2018, **8**, 1703401.
- 13 M. Jevric, A. U. Petersen, M. Mansø, S. K. Singh, Z. Wang, A. Dreos, C. Sumby, M. B. Nielsen, K. Börjesson, P. Erhart, and K. Moth-Poulsen., *Chem. Eur. J.*, 2018, **24**, 12767–12772.
- 14 A. U. Petersen, M. Jevric and K. Moth-Poulsen., *Eur. J. Org. Chem.*, 2018, **32**, 4465–4474.
- 15 A. Vlasceanu, S. L. Broman, A. S. Hansen, A. B. Skov, M. Cacciarini, A. Kadziola, H. G. Kjaergaard, K. V. Mikkelsen and M. B. Nielsen, *Chem. Eur. J.*, 2016, **22**, 10796–10800;
- 16 M. Cacciarini, A. B. Skov, M. Jevric, A. S. Hansen, J. Elm, H. G. Kjaergaard, K. V. Mikkelsen and M. B. Nielsen, *Chem. Eur. J.*, 2015, **21**, 7454–7461.
- 17 M. Cacciarini, M. Jevric, J. Elm, A. U. Petersen, K. V. Mikkelsen and M. B. Nielsen, *RSC Adv.*, 2016, **6**, 49003–49010.
- 18 O. Schalk, S. L. Broman, M. Å. Petersen, D. V. Khakhulin, R. Y. Brogaard, M. B. Nielsen, A. E. Boguslavskiy, A. Stollow and T. I. Sølling, *J. Phys. Chem. A*, 2013, **117**, 3340–3347.
- 19 A. B. Skov, S. L. Broman, A. S. Gertsen, J. Elm, M. Jevric, M. Cacciarini, A. Kadziola, K. V. Mikkelsen and M. B. Nielsen, *Chem. Eur. J.*, 2016, **22**, 14567–14575.
- 20 Z. Wang, J. Udmark, K. Börjesson, R. Rodrigues, A. Roffey, M. Abrahamsson, M. B. Nielsen and Kasper Moth-Poulsen, *ChemSusChem*, 2017, **10**, 3049–3055.
- 21 M. H. Hansen, S. T. Olsena, K. O. Sylvester-Hvidb and K. V. Mikkelsen, *Chem. Phys.*, **519**, 92–100.
- 22 R. R. Islagulov and F. N. Castellano, *Angew. Chem., Int. Ed.*, 2006, **45**, 5957–5959.

- 23 K. Edel, X. Yang, J. S. A. Ishibashi, A. N. Lamm, C. Maichle-Mössmer, Z. X. Giustra, S. Liu and H. F. Bettinger, *Angew. Chem., Int. Ed.*, 2018, **57**, 5296–5300.
- 24 H. Taoda, K. Hayakawa, K. Kawase and H. Yamakita, *J. Chem. Eng. Jpn.*, 1987, **3**, 265–270.
- 25 A. Natansohn and P. Rochon, *Chem. Rev.*, 2002, **102**, 4139–4175.
- 26 K. G. Yager and C. J. Barrett, *J. Photochem. Photobiol., A*, 2006, **182**, 250–261.
- 27 A. A. Beharry and G. A. Woolley, *Chem. Soc. Rev.*, 2011, **40**, 4422–4437.
- 28 J. Olmsted III, J. Lawrence and G. G. Yee, *Sol. Energy*, 1983, **3**, 271–274.
- 29 H. Taoda, K. Hayama, K. Kawase and H. Yamashita, *J. Chem. Eng. Jpn.*, 1987, **20**, 265–270.
- 30 A. Natansohn and P. Rochon, *Chem. Rev.*, 2002, **102**, 4139–4175.
- 31 K. G. Yager and C. J. Barrett, *J. Photochem. Photobiol. A: chem*, 2006, **182**, 250–261.
- 32 A. A. Beharry and G. A. Woolley, *Chem. Soc. Rev.*, 2011, **40**, 4422–4437.
- 33 M. Irie, *Bull. Chem. Soc. Jpn.*, 2008, **81**, 917–926.
- 34 A. M. Kolpak and J. C. Grossman, *Nano Lett.*, 2011, **11**, 3156–3162.
- 35 A. M. Kolpak and J. C. Grossman, *J. Phys. Chem.*, 2013, **138**, 034303
- 36 T. J. Kucharski, N. Ferralis, A. M. Kolpak, J. O. Zheng, D. G. Nocera and J. C. Grossman, *Nat. Chem.*, 2014, **6**, 441–447.
- 37 I. Gui, K. Sawyer and R. Prasher, *Science*, 2012, **335**, 1454–1455.
- 38 L. C. Branco and F. Pina, *Chem. Commun.*, 2009, **0**, 6204–6206. 643.
- 39 Zhang, S. Liu, Q. Zhang and Y. Deng, *Chem. Commun.*, 2011, **47**, 6641–6.
- 40 G.D Han, S.S Park, Y. Liu, D. Zhitomirsky, E. Cho, M. Dinca and J.C. Grossman, *J. Mater. Chem. A*, 2016, **4**, 16157–16165.
- 41 D. Zhitomirsky and J. C Grossman, *ACS Appl. Mater. Interfaces*, 2016, **8**, 26319–26325.
- 42 D. Zhitomirsky, E. Cho, and J. C Grossman, *Adv. Energy Mater.*, 2016, **6**, 1502006.
- 43 K. Masutani, M-a. Morikawa and N. Kimizuka, *Chem. Commun.*, 2014, **50**, 15803–15806.
- 44 K. Stranius and K. Börjesson, *Sci. Rep.*, 2017, **7**, 41145.
- 45 J. A. Bouwstra, V. V. De Leeuw and J. C. Van Miltenburg, *J. Chem. Thermodynam.*, 1985, **17**, 685–695.
- 46 E. Titov, L. Lysyakova, N. Lomadze, A.V. Kabashin, P. Saalfrank, and S. Santer, *J. Phys. Chem. C*, 2015, **119** (30), 17369–17377.
- 47 A. Cembran, F. Bernardi, M. Garavelli, L. Gagliardi, G. Orlandi, *J. Am. Chem. Soc.*, 2004, **126**, 3234–3243.
- 48 A. Goulet-Hanssens, M. Utecht, D. Mutruc, E. Titov, J. Schwarz, L. Grubert, D. Bléger, P. Saalfrank, and S Hecht., *J. Am. Chem. Soc.*, 2017, **139**, 335–341.
- 49 M. Cacciarini, A. Vlasceanu, M. Jevric and M. B. Nielsen, *Chem. Commun.*, 2017, **53**, 5874.
- 50 H. M. D. Bandara and S. C. Burdette., *Chem. Soc. Rev.* 2012, **41** (5), 1809–1825.
- 51 C. García-Iriepa, M. Marazzi, L. M. Frutos, D. Sampedro, *RSC Adv.*, 2013, **3**, 6241–6266.
- 52 H. M. Dhammika Bandara, S. C. Burdette, *Chem. Soc. Rev.*, 2012, **41**, 1809–1825.
- 53 J. Moreno, L. Grubert, J. Schwarz, David Bléger, S. Hecht., *Chem.Eur.J.*, 2017, **23**, 14090–14095.